

國立臺灣大學理學院海洋研究所

碩士論文

Graduate Institute of Oceanography

College of Science

National Taiwan University

Master Thesis

浮游食物網中跨營養階層攝食行為對於體型大小頻譜
之影響

Size spectrum is critically affected by omnivorous and
detritivorous feeding in plankton food webs



張俊偉

Chun-Wei Chang

指導教授：謝志豪 博士 Chih-hao Hsieh, Ph.D.

三木健 博士 Takeshi Miki, Ph.D.

中華民國 98 年 6 月

June, 2009

Contents

Contents	I
Abstract	III
中文摘要	IV
Introduction	1
The importance of body size in ecosystem research	1
The ecological metabolic theory	1
About size spectrum	2
Theoretical models on size spectrum	3
Examination of size-trophic level relationship	4
A case study in the Feitsui Reservoir	5
Methods and materials	7
<i>Sample collection</i>	7
<i>Size spectrum analyses</i>	8
<i>Stable isotope analysis</i>	9
<i>Physical, chemical and other biotic data</i>	10
Data Analysis	11
<i>Trophic level (TL) estimation</i>	11
<i>Size spectrum</i>	14
Results	17
Isotope data ordination and grouping	17
The size-TL relationship	17
Energy mobilization in Feitsui Reservoir	18
Residual analysis of size spectrum	19
Discussion	21
Size-TL relationship	21
<i>Coexistence of two food chains in microbial food web</i>	21
<i>Inversed size-TL relationship</i>	23
<i>Negative trophic position problem</i>	24
Size spectrum	25
<i>Residual analysis</i>	25

<i>The evaluation of ecological metabolic theory</i>	27
Energetic mobilization modes in Feitsui reservoir	29
Conclusion	30
Figure Reference	31
Table Reference	32
Figure	33
Table.....	46
Appendix.....	60
Derivation TE, size spectrum, PPMR relationship	60



Abstract

One of the most important issues in environmental conservation and ecosystem management is to develop good indices for efficiently monitoring ecosystems. Size spectrum is one of the potential candidate indices and has often been used as an index to detecting functional processes in aquatic ecosystems. However, the mechanism for formation of size spectrum is still under debate. Most theoretical models concerning size spectrum assume a linear relationship between log size and trophic level (size-TL relationship). However, this linear size-TL relationship in microbial food webs has not been examined. In this study, we examined the size-TL relationship and structure of size spectrum under different size-TL relationships. To do so, we sampled time series of plankton size spectra from Feb. 2008 to Feb. 2009 in the Feitsui Reservoir and carried out size fractionated stable isotope analyses. We found that the linear size-TL relationship does not always exist in the microbial ecosystem of the Reservoir, possibly due to the following two factors: (1) the extent of energy contribution from microbes and larger phytoplankton to higher trophic levels, and (2) the omnivorous interactions between zooplankton and microbes. The weak size-TL relationship caused the size spectrum to deviate from power-law distribution and intensify the secondary structure in size spectrum.

中文摘要

如何有效率地取得良好的指標用以監測生態系統功能為當今環境保護及生態系統管理的重大議題。在生態系統中，經常以個體的體型大小頻譜為監測水域生態系統的重要指標。然而，體型大小頻譜形成的機制至今仍未有定論，過去用以解釋體型大小頻譜的理論模式，皆假設經對數轉換的體型大小以及營養階層之間存在著一良好的線性關係，然而支持此假設的證據多侷限於由大型生物所形成之食物網，未考慮存在於微生物食物網中的各樣複雜交互作用可能會破壞此線性關係，因此本研究以碳氮穩定同位素分析來檢驗此基本假設，並調查當有違反此假設的情況時，體型大小頻譜結構會受到怎樣的影響。欲達此目的，本研究中收集了在翡翠水庫中浮游生物的體型大小頻譜的時間序列資料，自 2008 年 2 月至 2009 年 2 月。結果發現此線性關係的假設並非恆成立，且體型大小與營養階層的關係主要受下列二因子影響 (1) 微生物或是大型浮游藻類的能量貢獻差異；(2) 浮游動物跨營養階層取食行為，皆使得營養階層與體型大小的關係非預期顯著。而營養階層與體型大小之間的薄弱關係使得體型大小頻譜偏離理論預測的冪次分布，並強化了體型大小頻譜中的次級結構。

Introduction

The importance of body size in ecosystem research

Understanding the ecosystem properties that can reveal influences from anthropogenic impacts and climatic changes is one of the most urgent issues for ecosystem management and conservation (Cairns et al. 1993). A critical concern is to develop fast-get indicators with maximum information but minimum cost to monitoring ecosystems. Body size related indices are such candidates, because many important traits of organisms are determined by size, e.g. prey size, home range, metabolic rate and generation time (Peters 1986). To investigate ecosystem functional processes, such as trophic dynamics and food web structures, the size structure among individuals usually tells more than taxonomic identities (Jennings et al. 2002a), and size is also a possible surrogate for the so called niche value in food webs (Cohen et al. 1990).

The ecological metabolic theory

The relationship between body size and many biological properties, such as metabolic rate (Peters 1986) and population density (Damuth 1981), is usually

described by a power-law function. A general model was proposed by West *et al.* (1997), which was derived from fractal-like network properties in the vascular system of organisms. The further revised version of model (Gillooly *et al.* 2001) predicts an allometric scaling relationship among body size, temperature and kinetic energy in respect to metabolism, expressed as

$$B \sim M_I^{3/4} e^{-E/kT}$$

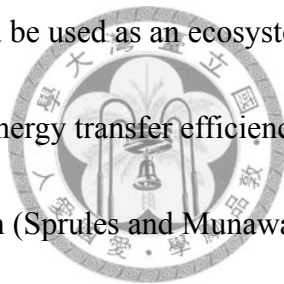
, where B is the metabolic rate, M is the body size, k is the Boltzmann constant, T is the absolute temperature, and E is the kinetic energy of the respiratory enzyme.

Many important ecosystem properties (e.g. production) and macroecological patterns (e.g. size spectrum) can be derived by this scaling metabolism-size relation (Brown *et al.* 2004). This metabolism-size relationship is the foundation of Ecological Metabolic Theory (MTE). One of the most important predictions of MTE at ecosystem level predicts that the slope of size spectrum is determined by averaged predator-prey size ratio (PPMR) and energy transfer efficiency (TE) (Brown *et al.* 2004) as **$\log TE / \log PPMR - 0.75$** (see appendix for the detail derivation).

About size spectrum

Size spectrum describes the relationship between each arbitrary size class and the corresponding abundance (or biomass) regardless of taxonomic identity (Sheldon *et al.*

1972). Size spectrum is one of the most well-known macroecological patterns in aquatic ecosystems (White et al. 2007). Since the first introduction by Sheldon in 1972, the similarity of size spectra among various ecosystems have been observed (Sprules et al. 1991, Modenutti and Balseiro 1994, Heath 1995), and one often found a linear relationship between size and abundance under logarithm scale known as power-law distribution. Power-law distribution is an essential property of complex networks (Barabasi and Albert 1999), such as ecological food webs (Montoya and Sole 2002). Because of such nonrandom and informative pattern of size spectrum, the structure of size spectrum could be used as an ecosystem indicator for revealing many ecosystem properties, such as energy transfer efficiency (Gaedke 1993, San Martin et al. 2006), perturbation detection (Sprules and Munawar 1986), and even be used in the calculation of fish yield (Kerr and Ryder 1988). For this reason, it is very important to understand the mechanisms underlying formation of power-law pattern in size spectrum.



Theoretical models on size spectrum

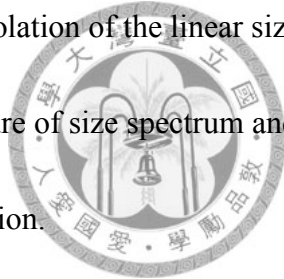
To date, there are two major theoretical models explaining the formation of size spectrum. One is the general predator/prey model of aquatic production (Silvert and Platt 1978, Kerr and Dickie 2001) derived from continuous mass and energetic flow

through size structured trophic levels. This model predicts power-law distribution with unspecified exponent. An alternative theoretical model, the MTE model, was derived from ecological metabolic theory. Despite that different mechanisms were proposed by these two theories, both of them agree a common assumption- a positive linear relationship between log body size and trophic level.

Examination of size-trophic level relationship

“The big eats the small” is a prevailing view in most of size spectrum models. Actually, abundant evidence (Cohen et al. 2003, Belgrano 2005) has shown that trophic level is linearly positive correlated with log transformed body size. Many theoretical models adopted this idea as their essential assumption (Silvert and Platt 1978, Kerr and Dickie 2001). While it is plausible to apply this relationship between size and trophic level (size-TL relationship) to all aquatic ecosystems, empirical evidence were only restricted to larger organisms but neglected the microbes. Does the linear size-TL relationship also exist in the microbial world where the structure of food web is more complicated than that of a grazing food web, particularly when considering the existence of microbial loop (Azam et al. 1983)? There are at least two possible caveats that might undermine this size-TL relationship in microbial food webs. First, when larger zooplankton omnivorously feeds on small microbes, the

trophic positions of zooplanktons may become nearly equal and independent of body size. The similar condition occur in not only microbial systems but also grazing food chain when large zooplankton omnivorously feeds on larger phytoplankton. Second, when energy flows from larger phytoplankton to smaller bacteria, nanoflagellate and ciliate, the relationship between size and trophic level is reversed. For these reasons, we proposed our hypothesis that the relationship between size and trophic level is weak or even nonexisistent in microbial systems because of the omnivorous interactions and microbial loop. Since this assumption is essential to the theoretical models of size spectrum, the violation of the linear size-TL relationship is expected to have an influence on the structure of size spectrum and cause the size spectrum to deviate from power-law prediction.

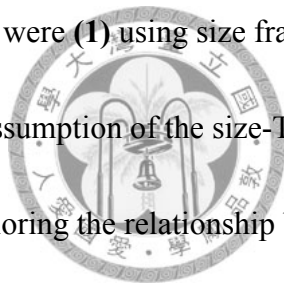


A case study in the Feitsui Reservoir

To investigate whether size spectrum is affected by feeding characteristics of predators, we carried out a time series sampling in the Feitsui Reservoir. The Feitsui Reservoir, located in the east-northern Taiwan and strictly protected, is the most important reservoir for drinking water source for the Taipei city, the capital of Taiwan. Therefore, monitoring and studying this ecosystem not only gives useful information for the water quality management but also provide an ideal system for scientific

research. Several microbial parameters (such as primary production (PP), bacterial production (BP), community respiration (CR) and algal composition), and many physical parameters and chemical parameters have been measured with a high frequency in a long-term program (Shiah, unpublished data; (Wu and Chou 1998, Kuo et al. 2003). However, trophic interactions in this pelagic ecosystem and zooplankton top-down effects were still unknown. Therefore, the Fetsui Reservoir provides an ideal system to study these important size-related issues.

The purposes of this study were **(1)** using size fractionated isotope analyses to construct and check the basic assumption of the size-TL relationship for plankton (Jennings et al. 2002b), **(2)** exploring the relationship between size-TL relationship and the structure of size spectrum, and **(3)** describing the size structured energy flows and trophic interactions of the pelagic ecosystem in the Feitsui Reservoir.



Methods and materials

Sample collection

In order to examine the size spectrum and size-TL relationship, sampling was carried out in the Feitsui Reservoir in Taipei, Taiwan, from February 2008 to February 2009. The location of sampling station is in an open area nearby the dam (Fig. 1). The plankton sample were collected by a 50- μm mesh plankton net and water samples by go-flow bottle every week when surface water temperature was higher than 20 °C and every other week when temperature was lower than 20 °C. For net sampling, a 50- μm mesh zooplankton net was towed vertically from the 50 m depth to the surface and the total volume of water passing through the net was calculated based on a flowmeter.

The sampling water column was usually aerobic in any time of this subtropical reservoir and without strong turbulent below 70 m depth. For water sampling, the samples were collected by go-flow bottle from 0, 5, 10, 15 and 20 meter depth and chlorophyll *a* maximum layer which can be known in advance through an automatic monitoring CTD. The samples collected from the Feitsui Reservoir were processed for two different purposes, size spectrum analysis and stable isotope analysis.

Size spectrum analyses

For zooplankton larger than 300 μm , half of the sample from 50- μm mesh nets was preserved with formalin of 2% final concentration and processed as the following procedures. First, a subsample constituted of roughly 300 individuals was taken from formalin preserved samples by micropipette, and the abundance of zooplankton was quantified. Second, all subsampled individuals were identified to the species level under microscope. Third, the length and width of each individual was measured by image analysis software under microscopic CCD.

For planktons ranging from 300 μm to 50 μm , net samples was loaded into a 300- μm flowcell in FlowCAM and observed under 10X objective lens. In FlowCAM, the pictures of all particles were taken and several basic image parameters (e.g. length and ESD) were measured. Finally, all abiotic images were manually removed.

For planktons ranging from 35 μm to 3 μm , mixed water sample from a mixture of five depths (0, 5, 10, 15 and 20 m) was analyzed by FlowCAM. All procedures for FlowCAM analyses followed the aforementioned protocol, except that the flowcell was changed to 50 μm and samples were observed under 20X objective lens. By compiling size-abundance data from FlowCAM analyses and microscopic measurements, plankton size spectra in the Feitsui Reservoir could be constructed for each sampling date.

Stable isotope analysis

For the isotope sample preparation, net samples and 5 liter water samples from the chlorophyll *a* maximum layer was kept for 1 to 2 hours for cleaning the gut content of zooplankton and then passed through 500, 177, 74, 44 and 10 μ m metal meshes and divided into 6 size fractionations. All plankton were washed down from metal meshes and filtered onto 0.7 glass fiber filter papers and then preserved in a -20°C freezer. Following such procedures, we obtained six size fractionated samples for each sampling date: **(1) >500, (2) 500-177, (3) 177-74, (4) 74-44, (5) 44-10 and (6) 10-0.7**. The main composition for each size fraction was shown in Table 1, which can be inferred from the FlowCAM images, microscopic observations, and the literature (Wetzel 2001). The six preserved size fractionated samples were dried out on freeze-dry machine. In order to remove inorganic carbonate, each sample was acid-treated with 1N HCl on pre-combusted (500 °C) glass and incubated in oven under 50 °C for 1-2 days. After acidic treatment, samples were incubated in desiccators at room temperature for at least one day. About 1.3 mg for each size fraction was packed into a tin capsule to determine carbon and nitrogen isotopic ratio in a Micromass VG602E mass spectrometer. Results were presented in the standard δ notation with respect to standards of atmospheric nitrogen and PDB carbon:

$$\delta^{13}\text{C} \text{ or } \delta^{15}\text{N} (\text{‰}) = (R_{\text{sample}} / R_{\text{standard}} - 1) \times 1000$$

where $R = {}^{15}\text{N} / {}^{14}\text{N}$ or ${}^{13}\text{C} / {}^{12}\text{C}$.

Physical, chemical and other biotic data

The variables include:

BB: bacterial abundance.

DO: dissolve oxygen.

Sal: salinity.

Temp: temperature.

Si: silica.

NO₂: Nitrite.

NO₃: Nitrate.

PO₄: phosphate.

Crus: The total biomass of crustacean.

Rot: the biomass of rotifer

PP: total primary production of euphotic zone



Except for the zooplankton variables and PP, all these variables were measured by trapezoidal integration average from 20 m depth to surface, the euphotic zone in the Feitsui Reservoir. Except for the biomass of rotifer and crustacean, all data were

available from Dr. Shiah's lab, Research Center for Environmental Changes,
Academia Sinica.

Data Analysis

Trophic level (TL) estimation

Sample size problem

For each sampling date, only 6 size fractions were included. Such sample size is too small to precisely estimate regression coefficients. To solve this statistical problem, we carried out data clumping. Twelve variables, $\delta^{15}\text{N}$ and $\delta^{13}\text{C}$ each of 6 size fractions, were used for multivariate clustering. By using K means clustering (Legendre 1998), data were grouped based on similar isotopic signatures. The number of groups was determined by maximizing the ssi index. In order to link K means groups to environmental factors, canonical redundancy analysis (RDA) (Legendre 1998) was carried out.

Trophic position estimation

In order to construct the size-trophic level relationship, the trophic level with

respect to the baselines of each size fraction was estimated. It is known that there are two organic carbon sources in the Feitsui Reservoir ecosystem, the **(4)74-44 μ m** and **(6)10-0.7 μ m** size fraction, which could be clearly identified in the $\delta^{15}\text{N}$ and $\delta^{13}\text{C}$ signature. Therefore, the **(4)74-44 μ m** and **(6)10-0.7 μ m** size fraction were assumed to be the baselines for other size fractions. This assumption is also supported by the images taken from FlowCAM analyses, which show that the **(4)74-44 μ m** size fraction is composed of larger phytoplankton. For this reason, obtaining the correct trophic level could be done by considering the two baselines at the same time. To do so, first, we formulated the relationship between the trophic level of the target size fraction TL_i and the trophic levels of baselines 4 and 6 is in the following equation

$$TL_i = f_4 TL_4^i + f_6 TL_6^i \text{-----} (*)$$

,where the TL_4^i and TL_6^i are the trophic level of baseline 4 and 6 respectively; f_4 and f_6 are relative contributions from baseline 4 and 6 respectively. Second, the isotope values of the target could be expressed by the weighted average of isotope values of baselines plus the trophic enrichments as the following equations

$$\delta^{13}C_i = f_4 (\delta^{13}C_4 + \varepsilon_c TL_4^i) + f_6 (\delta^{13}C_6 + \varepsilon_c TL_6^i)$$

$$\delta^{15}N_i = f_4 (\delta^{15}N_4 + \varepsilon_n TL_4^i) + f_6 (\delta^{15}N_6 + \varepsilon_n TL_6^i)$$

,where $\delta^{13}C_i$ and $\delta^{15}N_i$ are the isotope values of the target fraction and ε_c & ε_n specified as 1 ‰ and 3.4 ‰ (Post 2002) is the trophic enrichment factor of $\delta^{13}\text{C}$ and

$\delta^{15}N$, respectively. By substituting the equation (*) into the two equations, we can get the following two equations

$$\delta^{13}C_i = f_4 \delta^{13}C_4 + f_6 \delta^{13}C_6 + \varepsilon_c TL_i \text{----- (a)}$$

$$\delta^{15}N_i = f_4 \delta^{15}N_4 + f_6 \delta^{15}N_6 + \varepsilon_n TL_i \text{----- (b)}$$

Under the constraint that the sum of two relative contribution should equal 1,

$$f_4 + f_6 = 1 \text{----- (c)}$$

The unknown trophic level, TL_i , could be estimated by solving the equation system (a), (b) and (c). To cancel out the assumed trophic enrichment factor, ε_n , the trophic

position TP_i was defined as $\varepsilon_n TL_i$ and used in the size-TL relationship estimation. As

we are interested in the slope of size-TL relationship, a constant trophic enrichment factor does not affect our results.



The relationship between size and trophic level

Ranged major axis linear regression analysis (RMA) were used to estimate the regression coefficients of the size-TL relationship because there is no predetermined dependent and independent variable (Legendre 1998). The RMA statistical model of the size-TL relationship could be expressed as the following equations:

$$(\delta^{15}N_i - \delta^{15}N_{base\ i}) = a + b \log_2 (W_i)$$

, where W_i is the weighted average size of the i th size fraction. W_i was computed from

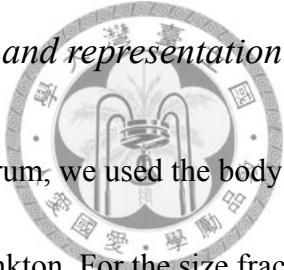
the distribution of biomass within each size fraction and expressed as the following equation:

$$W_i = \frac{\beta+2}{\beta+3} \frac{W_{U_i}^{\beta+3} - W_{L_i}^{\beta+3}}{W_{U_i}^{\beta+2} - W_{L_i}^{\beta+2}}$$

, where the β is the slope of the empirical size spectrum; W_{U_i} and W_{L_i} is the upper bound and lower bound of the i th size fraction, respectively.

Size spectrum

Size spectrum construction and representation



To construct the size spectrum, we used the body volume in the unit of μm^3 as the measure of body size of plankton. For the size fraction ranging from 3 to 300 μm , the body volume was estimated by ESD (Equivalent Spherical Diameter) of the images obtained from FlowCAM. For the zooplankton larger than 300 μm , taxon-specific empirical length-volume transformation was used to estimate zooplankton body volume. After obtaining the body size data for all individuals, the planktons were grouped into size classes according to their body volume. The i th size class (S_i) was defined as the interval of 2 to the integer powers i and $i-1$, $(2^{i-1}, 2^i]$ (μm^3), which constitute the x-axis of size spectrum. Then the accumulated bio-volume (V_i) for each corresponding size class S_i was computed and divided by the

corresponding size class band width (bw_i), known as normalization (Platt and Denman 1978). Finally, the statistical model of size spectrum to fit the general predator/prey model is expressed as the following equation:

$$\log_2(V_i / bw_i) = \alpha + \beta \log_2(\text{midpoint}(S_i))$$

, where the α & β are unspecified intercept and slope.

Residual analysis of size spectrum

From the theories of size spectrum under steady state, the general predator prey model (Kerr and Dickie 2001) predicts that size spectrum should follow a power-law distribution without a specified exponent, while the MTE model (Brown and Gillooly 2003) predicts a power-law distribution with an exponent equal to -1, assuming that the TE and PPMR are 10% and 10^4 , respectively. To test the hypothesis that the weak size-TL relationship might lead the size spectrum to deviate from model predictions, either from the general predator/prey model or MTE model, two kinds of residuals were computed to quantify the extent of deviation. The first type of residuals, e_1 , was used to quantify the extent of deviation of size spectrum from the general predator/prey model prediction, which could be calculated from the difference between empirical \log_2 total biovolume Y , and general predator/prey model predicted \log_2 total biovolume Y' , $e_1 = Y - Y'$. The estimator of Y' could be obtained from

statistical general predator/prey model. The second type of residuals, e_2 , was used to quantify the extent of deviation from the MTE model, which was measured by the difference between empirical \log_2 total biovolume Y and MTE model predicted \log_2 total biovolume Y^* , $e_2 = Y - Y^*$. The estimator of Y^* could be estimated by fitting the empirical size spectrum into the following statistical linear model

$$Y^* = \log_2(V_i / bw_i) = \alpha - \log_2(\text{midpoint}(S_i))$$

where the intercept α could be estimated by the sample mean of $(Y + \log_2(\text{midpoint}(S_i)))$. Those residuals were analyzed by the residual plot and polynomial local weighting regression analysis (cubic spline).



Results

Isotope data ordination and grouping

K means clustering showed that six groups could be identified by maximizing the ssi index (Fig. 2& Table 2), denoted as A, B, C, D,E, and F. The grouping determined by K means clustering is also consistent with the result of RDA ordination (Fig. 3). The determination of groups can be largely explained by environmental variables (permutation test, $p < 0.001$, Table 3).



The size-TL relationship

The regression analysis indicates that only 7 among the 24 sampling dates have a significant size-TL relationship (Table 4), likely due to small sample size. After data lumping, three (B, E and F) of the six K means groups showed a significant size-TL relationship (Fig. 4b, 4e and 4f and Table 5). However, the R-square values were low in these groups (from 0.32 to 0.05). The persistent weakness of size-TL relationship may be caused by the persistent inversed size-TL relationship between the **(4)74-44 μm** and **(5)44-10 μm** size fractions. These results support our hypothesis that the relationship between size and trophic level are often weak or even nonexistent in

our microbial system. For exploring the factors affecting the significance of a size-TL relationship, we further compared the two K means groups: with a significant size-TL relationship (named the size-oriented feeding regime) versus without a significant size-TL relationship (named the size-unoriented feeding regime).

Energy mobilization in Feitsui Reservoir

By comparing the $\delta^{13}\text{C}$ distance between size-oriented feeding regime and size-unoriented feeding regime, the effect of the energy transfer from microbes to zooplankton on the size-TL relationship can be known. The $\delta^{13}\text{C}$ distance, $\Delta^{13}\text{C}_{ij}$, between the target size fraction *i* and the baseline fraction *j* was defined as $(\delta^{13}\text{C}_i - \delta^{13}\text{C}_j)^2$. As such, the trophic relationship between each size fraction and the two baseline fractions was inferred. Larger $\Delta^{13}\text{C}_{ij}$ means relatively less contribution from the baseline fraction *j* to the size fraction *i*. The result shows that the size-unoriented feeding regime have significantly larger $\Delta^{13}\text{C}_{i4}$ but significantly smaller $\Delta^{13}\text{C}_{i6}$, *i* = 1, 2 & 3 than the size-oriented feeding regime (Table 7). This result indicates that the microbes (the **(6)10-0.7 μm** size fraction) transfer more energy to the **(1) >500 μm** , **(2) 500-177 μm** and **(3)177-74 μm** size fractions than the large phytoplankton (the **(4) 74-44 μm** size fraction) in the size-unoriented feeding regime, suggesting that the energy transfer from microbes to zooplankton was related to the non-significance of

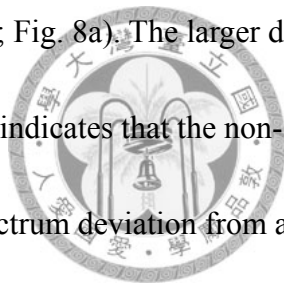
size-TL relationship. Moreover, the extent of the energy contribution from the two energy sources to zooplankton might be affected by the primary production in the ecosystem. The regression analysis of $\delta^{13}\text{C}$ distance to primary production showed that the $\Delta^{13}\text{C}_{14}$, $\Delta^{13}\text{C}_{34}$ and $\Delta^{13}\text{C}_{56}$ significantly increased with primary production (Fig. 5 & Fig. 6).

However, not only the use of microbial energy source but also the feeding behavior of zooplanktons might affect the significance of size-TL relationship. The result of ANOVA analysis shows that there is significant trophic position elevation from small zooplankton to larger zooplankton in size-oriented feeding regime but not in size-unoriented feeding regime (Table 8). In the size-unoriented feeding regime, the trophic positions of zooplankton are indistinguishable and $\delta^{13}\text{C}$ signatures among zooplankton and microbes are similar for most sampling dates (Fig. 10.). This implies that larger zooplankton feeds directly on microbes without involving small zooplankton as the intermediate agent, which is the omnivorous feeding.

Residual analysis of size spectrum

The size-TL relationship has effects on the structure of size spectrum. From the cubic spline analysis, the residuals of general predator/prey model and MTE model were significantly different from zero in the microbial part ($p < 0.05$). The positive maximum and negative maximum residuals occur in the **(5)44-10 μm** and **(4)74-44 μm**

size fraction respectively (Fig. 7), where the persistent inversed size-TL relationship occurs. Further comparison between size-oriented & size-unoriented feeding regimes shows that the mean sum of square of residuals in the **(4)74-44 μm** size fraction is significantly smaller than zero and significantly larger than zero in zooplankton fractions (the **(1) >500 μm** , **(2)500-177 μm** and **(3)177-74 μm** size fractions) in the size-unoriented feeding regime (Fig.9, $p < 0.05$) but not in the size-oriented feeding regime (Fig.9, $p > 0.05$). Moreover, the deviations of size spectrum of zooplankton showed a significant positive linear relationship to size in the size-unoriented feeding regime (slope = 0.179, $p < 0.001$; Fig. 8a). The larger deviation of size spectra in the size-unoriented feeding regime indicates that the non-significance of size-TL relationship may cause size spectrum deviation from a power-law distribution.



Discussion

Size-TL relationship

Coexistence of two food chains in microbial food web

The weak size-TL relationship in the microbial food web (Fig. 4) is consistent with our expectation that the complicated interactions between food chains lead to a weak size-TL relationship. The $\delta^{13}\text{C}$ distance analysis showed that the size-TL relationship was significant when zooplankton tend to consume large phytoplankton, the **(4)74-44 μm** size fraction. By contrast, when zooplankton tend to consume the **(6)10-0.7 μm** size fraction (dominated by bacteria, cyanobacteria and tiny phytoplankton), the size-TL relationship became non-significant. This result may be caused by the flattened slope of size-TL relationship because of the high predator-prey size ratio in zooplankton-microbe interaction.

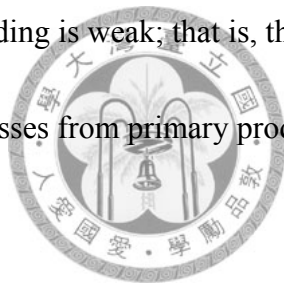
The extent of the energy contribution from the two sources to zooplankton is affected by primary production (Fig. 5 & Fig. 6), which is consistent with the fact that the small autotrophs (less than 10 μm) made more contribution to primary production than larger phytoplankton in the Feitsui Reservoir (unpublished data, Lai). As such, when primary production is high, the microbes pass more energy to zooplankton than

large phytoplankton. In other words, zooplankton use energy from different sources, depending on resource availability in this ecosystem. The other reason for zooplankton in the Feitsui Reservoir to consume less large phytoplankton might be that some dominant larger algae are often inedible because of the toxic content (such as *Microcystis spp.* and *Ceratium spp.*), spiny morphology (*Staurastrum spp.*) and digestion difficulty (e.g. the diatom frustules). However, the debris of the phytoplankton may be converted to edible materials through the decomposition pathway and later used by protists. The isotope analysis showed that the $\delta^{13}\text{C}$ signature of protists (the **(5)44-10 μm** size fraction, Fig. 10.) is similar with that of large phytoplankton, but their $\delta^{15}\text{N}$ are much higher than large phytoplankton in most of sampling dates. This detritivorous interaction between larger phytoplankton and protists results in a persistent inversed size-TL relationship in our dataset.

Omnivorous feeding behavior of zooplankton

The size-TL relationship depends on not only the energy sources used by zooplankton but also the pathway that zooplankton obtain the energy from the two energy sources. Under the size-unoriented feeding regime, zooplanktons regardless of their size exhibited a similar trophic position and $\delta^{13}\text{C}$ value (ANOVA, Table 8.). This is contrast to the size-oriented regime. This observation indicates that zooplanktons

feed directly on microbes without involving small zooplankton as the intermediate agent in the size-unoriented regime, known as omnivorous feeding (Sprules and Bowerman 1988). This direct feeding interaction between larger zooplankton and microbes prevalently exist in many aquatic ecosystems (Peterson et al. 1978, Knoechel and Holtby 1986, Brendelberger 1991). When zooplankton with different body sizes consumes the resources with similar size, there is no size-dependent feeding interaction. Consequently, the size-TL relationship tends to be non-significant as strong omnivory occurs. By contrast, the size-TL relationship is significant when the intensity of omnivorous feeding is weak; that is, the smaller zooplankton is the intermediate agent as energy passes from primary producers to large zooplankton.



Inversed size-TL relationship

Even though in some cases the size-TL relationship is significant, the relationship between body size and trophic level still remains weak in this microbial plankton food web. Here, we propose that the persistent weakness of size-TL relationship is due to the persistent inverse size-trophic level relationship in the Feitsui Reservoir. Such an inverse size-TL relationship can be found in the size fraction **(4)74-44 μ m** and **(5)44-10 μ m**, the larger phytoplankton and smaller protists. This result also implies that the ciliates or heterotrophic nanoflagellates do not always

exclusively use the energy from the smaller bacteria or cyanobacteria; instead, they can substantially use the energy from larger phytoplankton perhaps after phytoplankton are decomposed. This can be considered as a detritivous foodchain. The trophic interaction between protists and large phytoplankton are also related to primary production in this reservoir. The protists tend to use more energy from larger phytoplankton, especially when the primary production is high (Fig. 6a.).

Negative trophic position problem

The TL calculated from the mixing baseline method shows that 12 out of 96 data points were smaller than 0. The negative values of estimated TL in the **(5)44-10 μ m** size fraction was probably due to the complex detritus pathway during which the $\delta^{15}\text{N}$ fractionation of some microbial decomposition activities might happen. The negative values of estimated TL in **the (1)>500 μ m** size fraction may come from decoupling of generation times of the baselines and **(1)>500 μ m** size fraction. Specifically, the generation time of large zooplankton is much longer than its resource. Such a difference in generation time might cause that zooplankton to integrate longer period of isotope fluctuations than its short-lived resource. For this reason, the isotope composition of zooplankton and baselines are mismatched. This problem could be improved by more frequent sampling or baseline invariant measurement, e.g. amino acid isotope analysis (Hannides et al. 2009).

Size spectrum

Residual analysis

Even though the assumption of a positive linear relationship between size and trophic level is not always hold in the microbial world, the overall size spectrum still approximately follows a power-law distribution (high R^2 , Table 9). However, upon carefully investigating the structure of residuals, we observed that size spectrum significantly deviated from the power-law distribution predicted by general predator/prey model or MTE in some size fractions (Fig. 7.). Moreover, the deviations at the small size part of the spectrum ((**4**)**74-44 μm** , (**5**)**44-10 μm** and (**6**)**10-0.7 μm** size fractions) are always higher than at the large size part ((**1**)**>500 μm** , (**2**)**500-177 μm** and (**3**)**177-74 μm** size fractions) ($p < 0.001$; Fig. 7a and 7b). This result is consistent with our hypothesis that the microbial part of size spectrum tend to deviate from power-law distribution because of complex microbial interactions which in turn causes size-TL relationship to deviate from a positive linear relationship. The positive maximum residual always appeared in the (**5**)**44-10 μm** size fraction in most of the sampling dates regardless of the significance of size-TL relationship (Fig. 8a and 8b). This indicates that the persistent inverse size-TL relationship between the (**4**)**74-44 μm**

and **(5)44-10 μm** size fraction (Fig. 4) could cause high degree deviation from the power-law distribution throughout all the sampling dates. These results are consistent with our hypothesis that the greater deviation of size spectrum at small-size fractions is corresponding to the alerted size-TL relationship. And we further explore this influence by comparing the difference of structure of size spectrum of the size-oriented feeding regime and the size-unoriented feeding regime. The larger phytoplankton, the **(4)74-44 μm** size fraction, showed significant deviation from power-law distribution in size-unoriented feeding regime but not in size-oriented feeding regime. Moreover, the deviation in zooplankton size spectrum has the significant positive linear relationship with size (slope = 0.179, $p < 0.001$) in the size-unoriented feeding regimes (Fig. 8a); by contrast, such a relationship was not seen in the size-oriented feeding regime ($p = 0.128$) (Fig. 8b). Greater deviation in the size spectrum of the size-unoriented feeding regime happened when strong omnivorous feeding occurred. Importantly, intensity of negative residuals in the **(4)74-44 μm** size fraction and positive residuals in zooplankton spectrum increased simultaneously as omnivorous feeding occurred. These results suggest that omnivorous feeding in food web might generate a secondary structure of size spectrum, which is often observed in a form of parabolic curves in many aquatic ecosystems. Actually, the secondary structure of size spectrum can be clearly



represented in our data as standardized size spectrum (standardization of all size spectra to slope equal to 0 and the same intercept to group average. The right hand side of Figure 13 is K means groups A, C & D, which belong to the size-unoriented feeding regime. They all show a clear V shape in the (4)74-44 μm size fraction, which is the intersection of two parabolic curves, the characteristic of the secondary structure of size spectrum. By contrast, this characteristic did not show up in the size-oriented feeding regime (the left hand side of Figure 13) where the extent of omnivorous feeding is weak. Kerr and Dickie (2001) proposed that the generation of secondary structures was accompanied with a power-law size distribution, but their model remains under debate. Here, we propose an alternative explanation that the generation of secondary structure of size spectrum is driven by omnivorous and detritivorous feeding.



The evaluation of ecological metabolic theory

We found that while the size-TL relationship often does not follow the model assumption of size spectrum theory, the primary structure of size spectrum still approximately follows power-law distribution (Table 9.). This result means that there are other contributing factors for the maintenance of the power-law distribution of size spectrum. Could it be the self-metabolic constraint on each size fraction as the

MTE pointed? In the application of MTE, the transfer efficiency in ecosystem could be estimated by *PPMR* and the slope of size spectrum (eqn. 1). By checking this transfer efficiency estimate, which is said to be within the range [0, 1] and 10% conventionally, the MTE prediction for the structure of size spectrum could be revised. In this study, we estimated *PPMR* by 2 to the power of trophic enrichment factor of $\delta^{15}N$ divided by the slope of size-TL relationship, $2^{(3.4/b)}$ (Jennings et al. 2002b) and TE by substituting the estimated *PPMR* and the estimated slope of size spectra to equ. 1. From the results of TE estimation, the weak size-TL relationship may lead to unrealistic high estimates of *PPMR* in some data (group C and D) and the estimated TE could not get the reasonable values which is conventionally believed around 10%. Did this imprecision come from the imprecise *PPMR* estimation? The answer is probably no. Despite that we use the most convincing size-TL relationship which gets the reasonable *PPMR* (267011.9) and the R-square up to 0.7, the TE estimate is still much higher than previously suggested (51.7%). On the other hand, from the theoretical relationship that the MTE predicted, the slope of size spectrum should be always less than -0.75 (Fig. 12.); otherwise the TE will bigger than one. However, in one case of our data in March 11th, 2008, the slope of size spectrum was shallower than -0.75 and the TE estimate was up to 301%! Therefore, the relationship claimed by MTE among the slope of size spectrum, *PPMR* and TE should be checked further

by empirical TE measurements.

Energetic mobilization modes in Feitsui reservoir

Intuitively, a size-TL relationship and size spectrum should exist; however, only a few empirical studies have shown a clear relationship between them. In this study, we show that robustness of the linear size-TL relationship is critically affected by feeding characteristics of plankton. Specifically, it depends on whether a grazing food chain (phytoplankton-zooplankton linkage) or a microbial food web prevails. When the grazing food chain dominates, the energy passes from larger phytoplankton to small zooplankton and then to large zooplankton. Consequently, the size-TL relationship was strong and the size spectrum follows a strong power-law distribution (Fig. 11a). By contrast, when the microbial food web dominates, the intensity of omnivorous feeding was extremely strong and the energy from larger phytoplankton to zooplankton was weak. Under this condition, the size-TL relationship was weak and size spectrum tends to show a high degree deviation from the power-law distribution, which results in apparent secondary structure seen in plankton size spectrum (Fig. 11b).

Conclusion

Size-based approaches to study trophic dynamics in aquatic ecosystems hold some promises but need more clarification. Importantly the linear relationship between size and trophic level were not always strong, at least in the microbial part of ecosystems. The disrupted size-TL relationship may result from the omnivorous energy mobilization from microbial food chain, which could be influenced by primary production. The disrupted size-TL relationship caused the size spectrum to deviate from power-law distribution and form the secondary structure, especially under the condition when the omnivorous feeding interaction between microbe and zooplankton are strong.

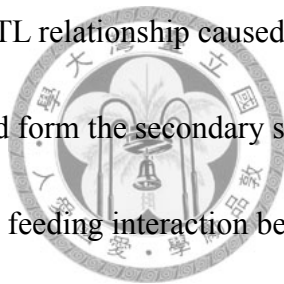


Figure Reference

Fig. 1. The map of Feitsui Reservoir

Fig. 2. The result of K means clustering

Fig. 3. RDA plot

Fig. 4. Size-TL relationship for K means groups

Fig. 5. PP- $\delta^{13}\text{C}$ distance (baseline 4) relationship

Fig. 6. PP- $\delta^{13}\text{C}$ distance (baseline 6) relationship

Fig. 7. Total residuals of general predator/prey model and MTE model

Fig. 8. Residual comparison between group with different size-TL structure

Fig. 9. Time series of $\delta^{15}\text{N}$ in Feitsui Reservoir

Fig. 10. Time series of $\delta^{13}\text{C}$ in Feitsui Reservoir

Fig. 11. Hypothetical energy mobilized models

Fig. 12. Theoretical relationship among transfer efficiency, PPMR and slope of size spectrum

Fig. 13. The standardized size spectrum

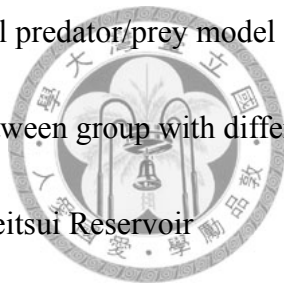


Table Reference

Table 1. Size fractions and their corresponding planktons

Table 2. Isotope data and their corresponding K means groups

Table 3. Permutation test of RDA

Table 4. Regression coefficients of size-TL relationship for each period

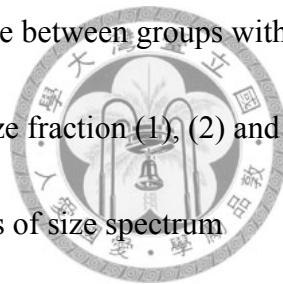
Table 5. Regression coefficients of size-TL relationship for six K means groups

Table 6. Regression coefficients of PP- $\delta^{13}\text{C}$ distance relationship

Table 7. $\delta^{13}\text{C}$ distance difference between groups with different sizeTL relationship

Table 8. ANOVA of $\delta^{15}\text{N}$ for size fraction (1), (2) and (3).

Table 9. Regression coefficients of size spectrum



Figure

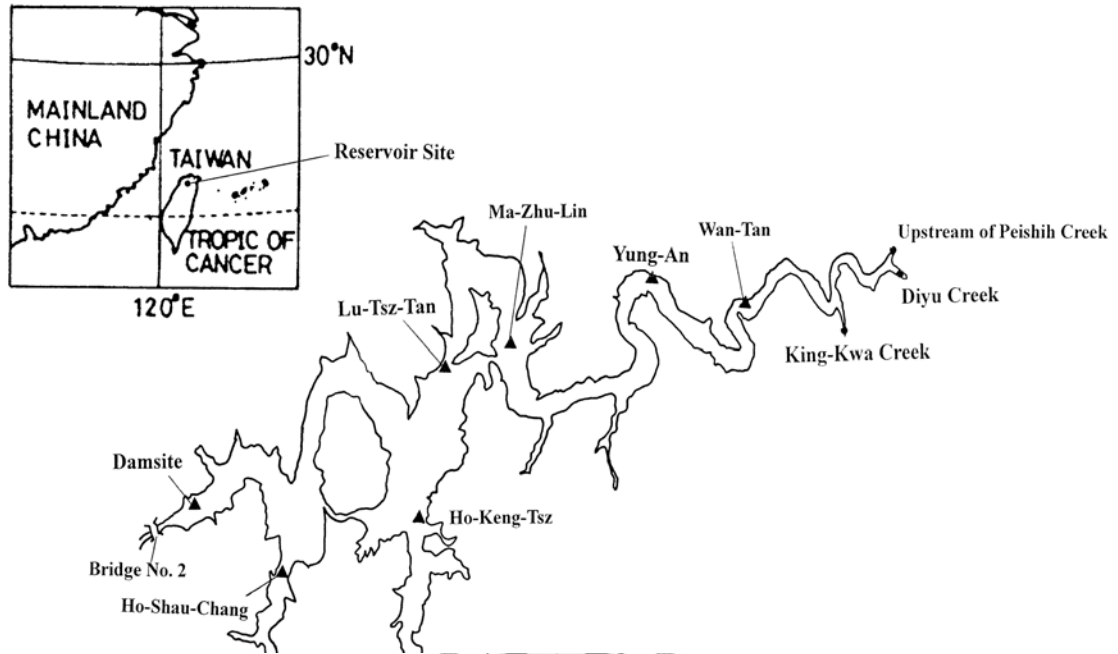
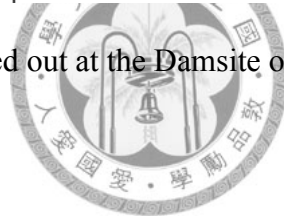


Figure 1 Sampling was carried out at the Damsite of the Feitsui Reservoir as shown in the map (Kuo et al. 2003).



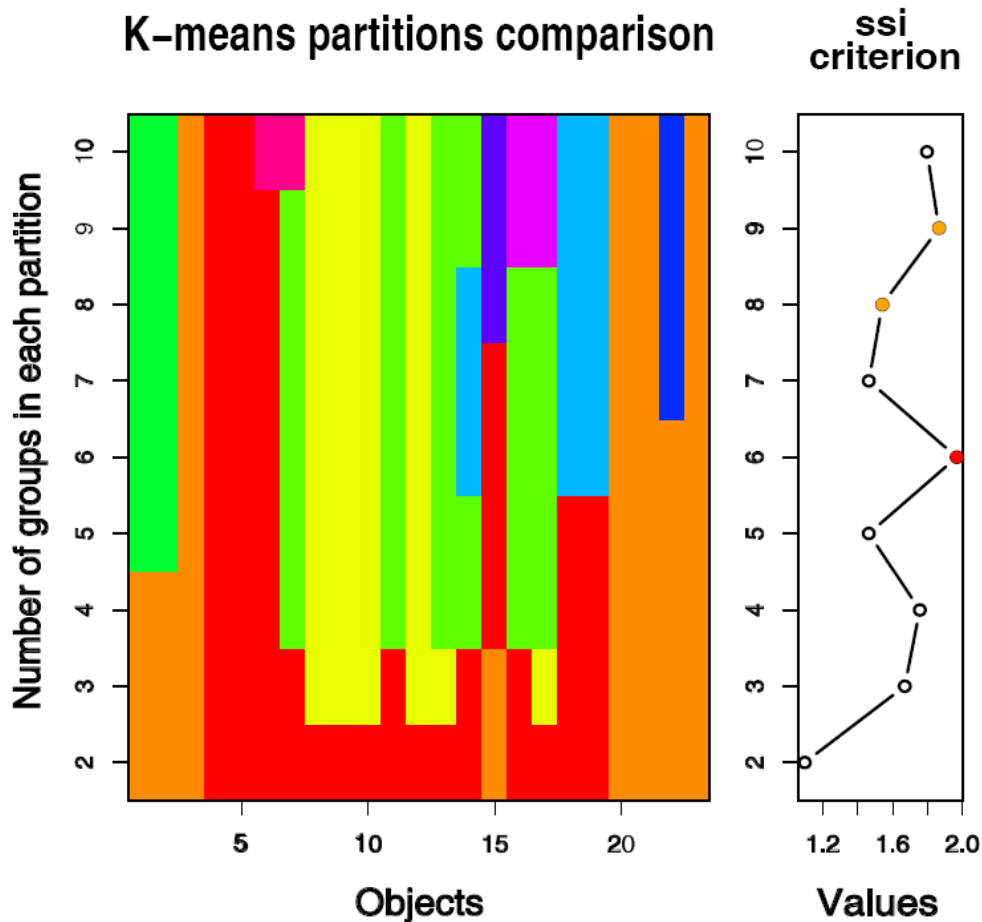


Figure 2 The result of K means cluster. The number of groups was determined by maximizing ssi criterion, the simple structure index which multiplicatively combine and normalize of the three components, maximum difference of each variable between the clusters, the sizes of the most contrasting clusters and the deviation of a variable in the cluster centers compared to its overall mean. There are six groups in this dataset could be identified by maximizing ssi criterion.

RDA of isotope structure

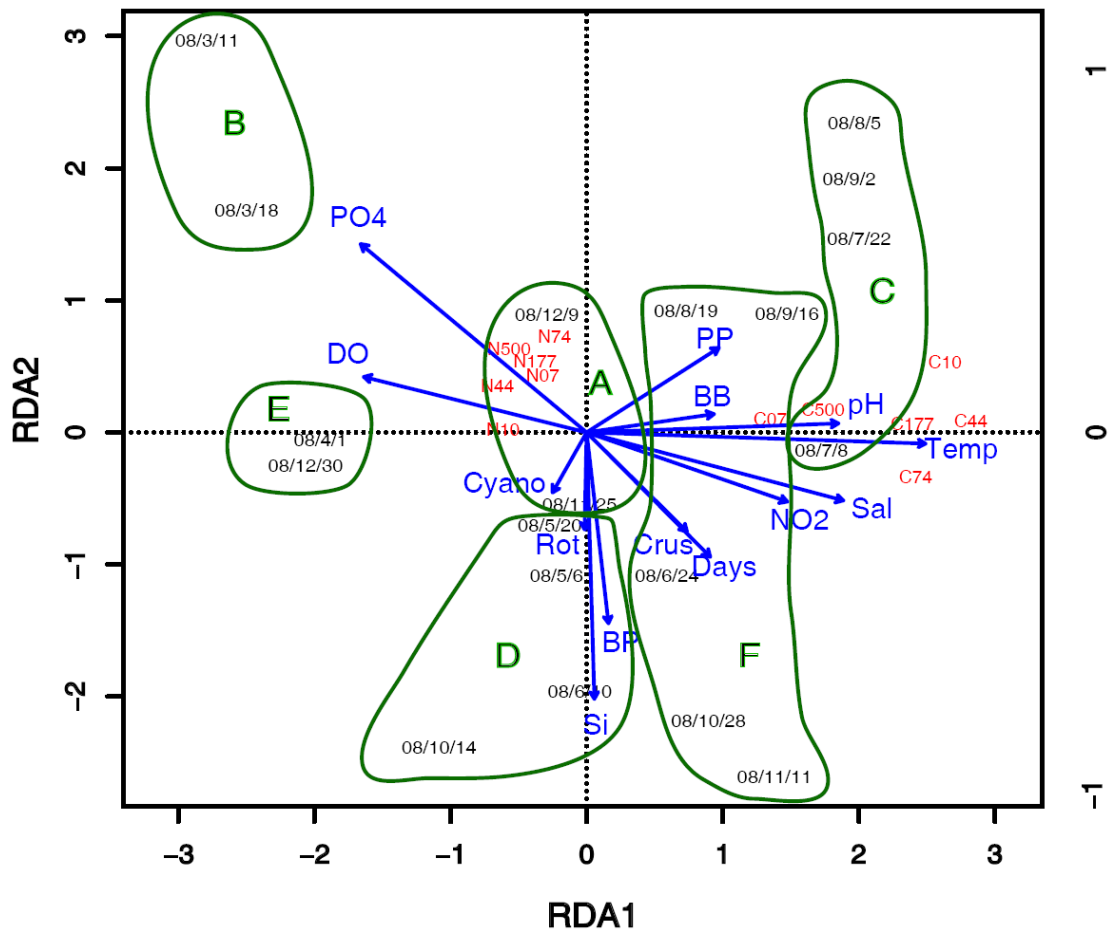


Figure 3 Biplot of canonical redundancy analysis. The variation of isotope data structure can be explained by those variables (permutation test, $p < 0.05$). RDA axis 1 and 2 can explain 82% of total variance of isotope data. The definition of abbreviations of variables was shown in the context. The groups A~F are the result of K means clustering.

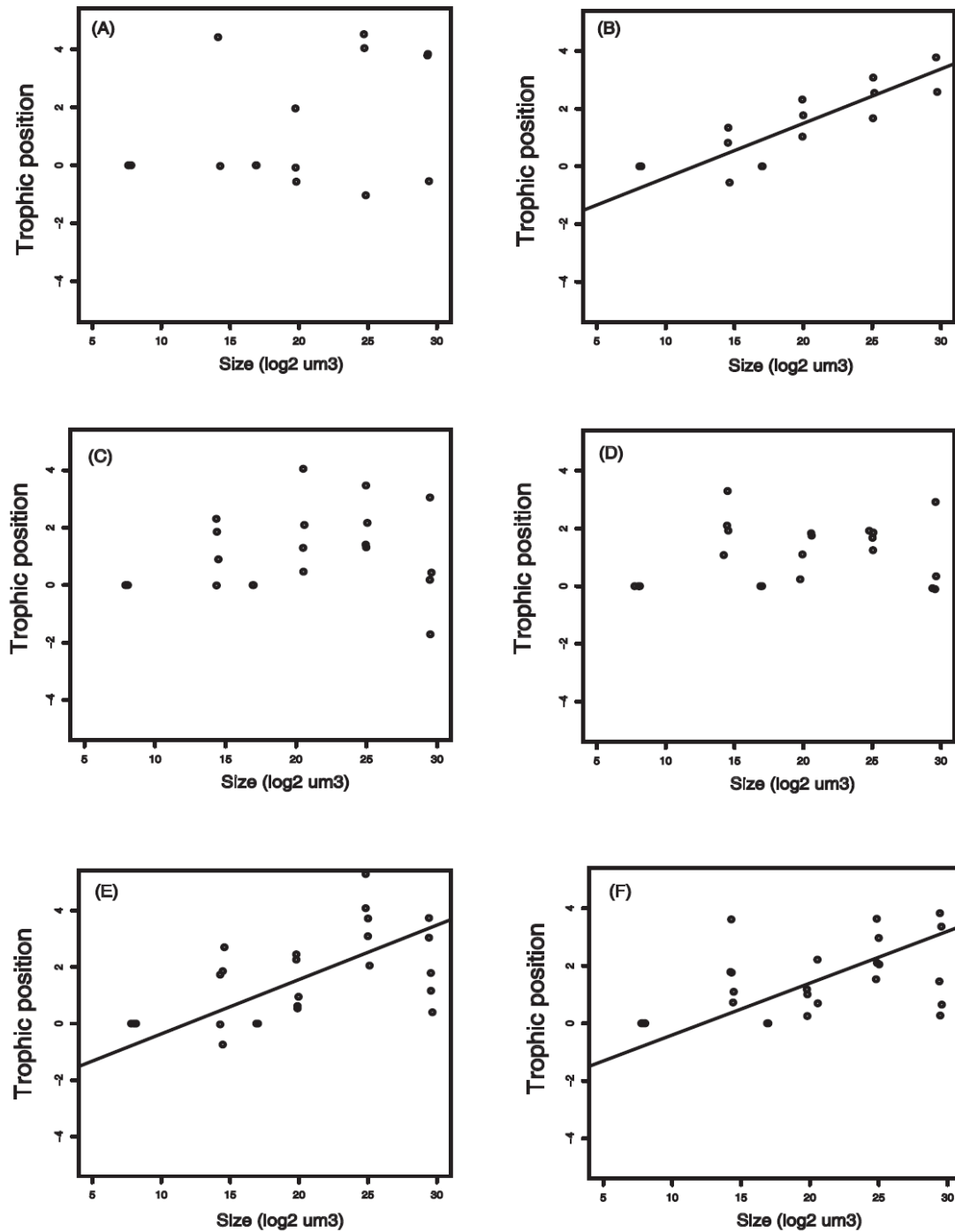
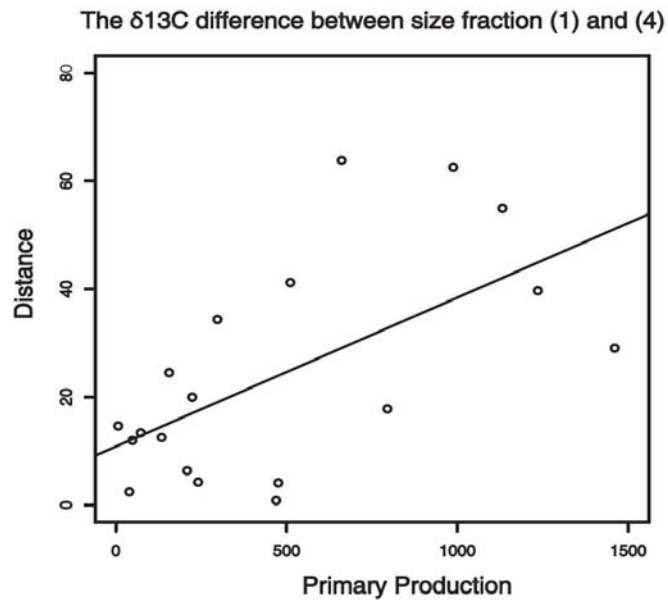


Figure 4 The relationships between size and trophic position in the six K means groups. The groups B, E and F show a significant size-TL relationship (permutation test, all p value <0.01); the groups A, C and D did not show a significant size-TL relationship (p value >0.1).

(a)



(b)

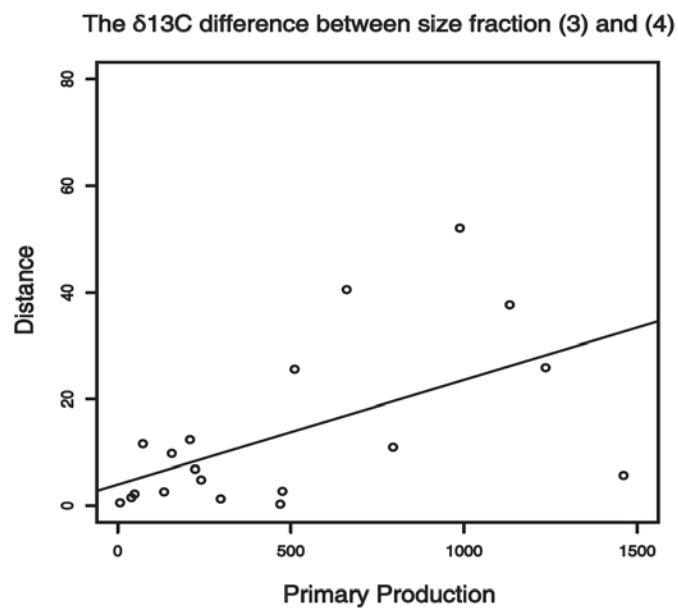
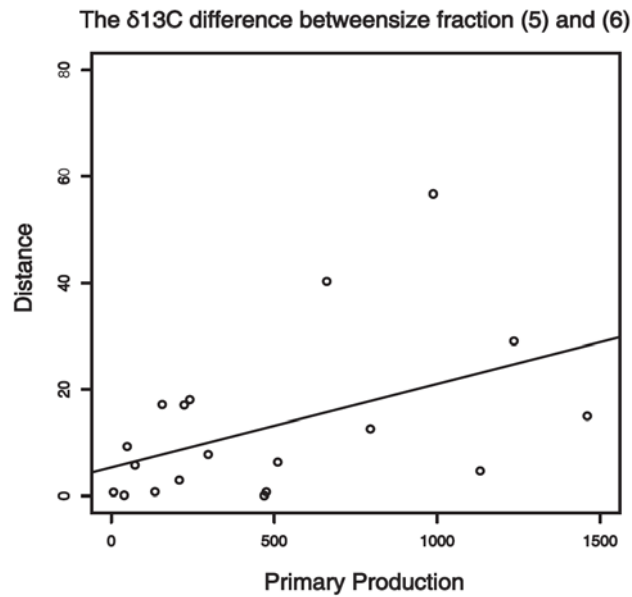


Figure 5 The significant relationship ($p < 0.05$) between primary production and $\delta^{13}\text{C}$ distance between (a) the (1)>500 μm size fractions and the (4)74-44 μm baseline fraction, and (b) the (3)177-74 μm size fraction and the (4)74-44 μm baseline fraction .

The result shows that the proportional use of larger phytoplankton of larger zooplankton might diminish with primary production increase.

(a)



(b)

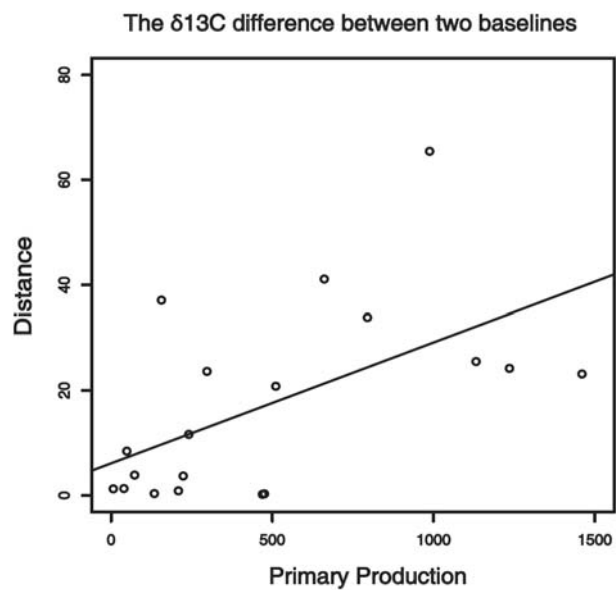
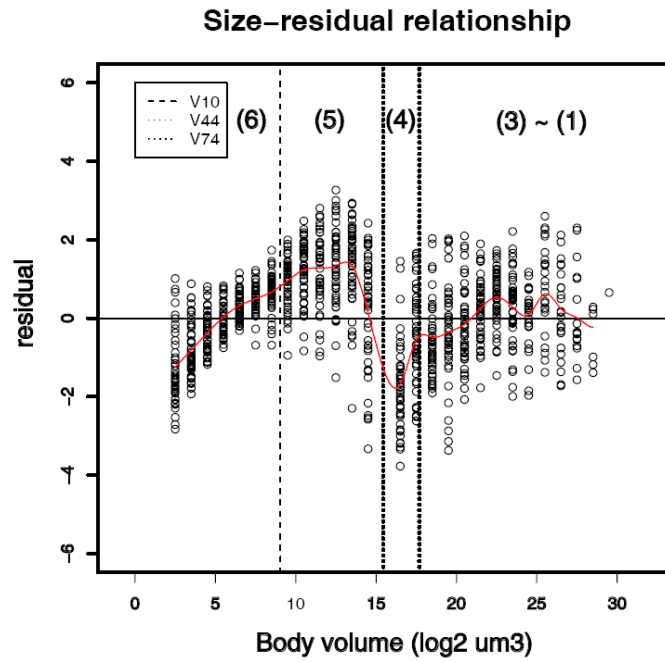


Figure 6 The significant relationship ($p < 0.05$) between primary production and $\delta^{13}\text{C}$ distance between (a) the (5)44-10 μm fraction and the (6)10-0.7 μm baseline fraction, and (b) between the (4)74-44 μm baseline fraction and the (6)10-0.7 μm baseline fraction. The result shows that the proportional use of smaller particle of smaller protists might diminish with primary production increase.

(a)



(b)

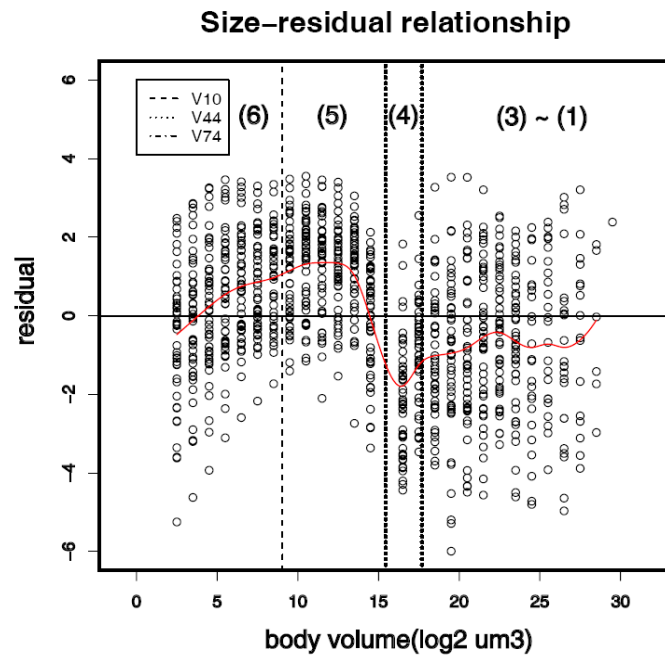
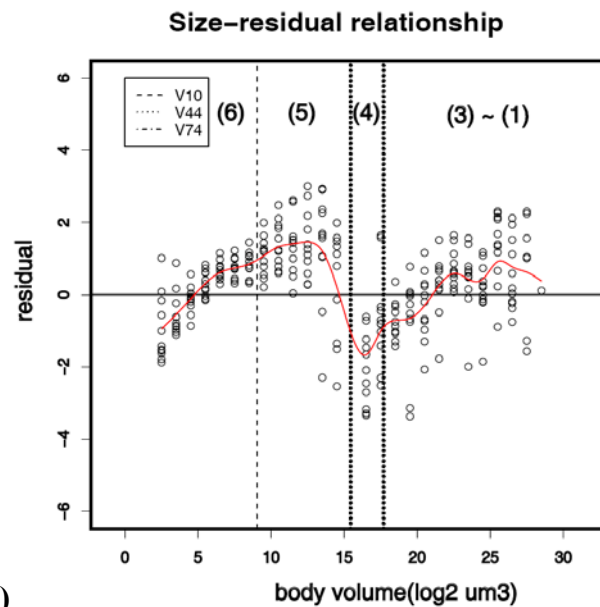
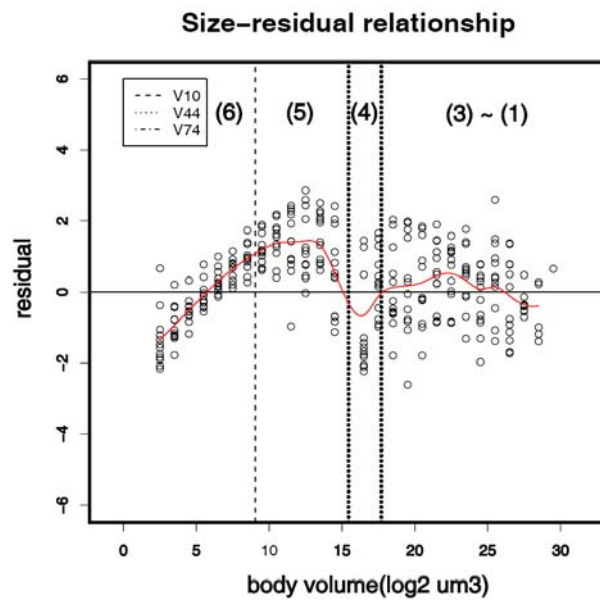


Figure 7 The relationship between size and (a) the residual from general predator/prey model (b) the residual from MTE model (power distribution with -1 exponent). Both kinds of residuals were all higher (red smoothing lines) in smaller particles, size fraction (4), (5) and (6), than zooplanktons, size fraction (1), (2) and (3)

(a)



(b)

Figure 8 The relationship between size and the residual from general predator/prey model in **(a)** groups showing a significant size-TL relationship **(b)** groups showing no significant size-TL relationship. Size spectrum is affected by the size-TL relationship. The residual in the **(4)74-44 μm** size fraction are significantly higher in groups showing no significant size-TL relationship.

The time series of $\delta^{15}\text{N}$ signature for all size fractions

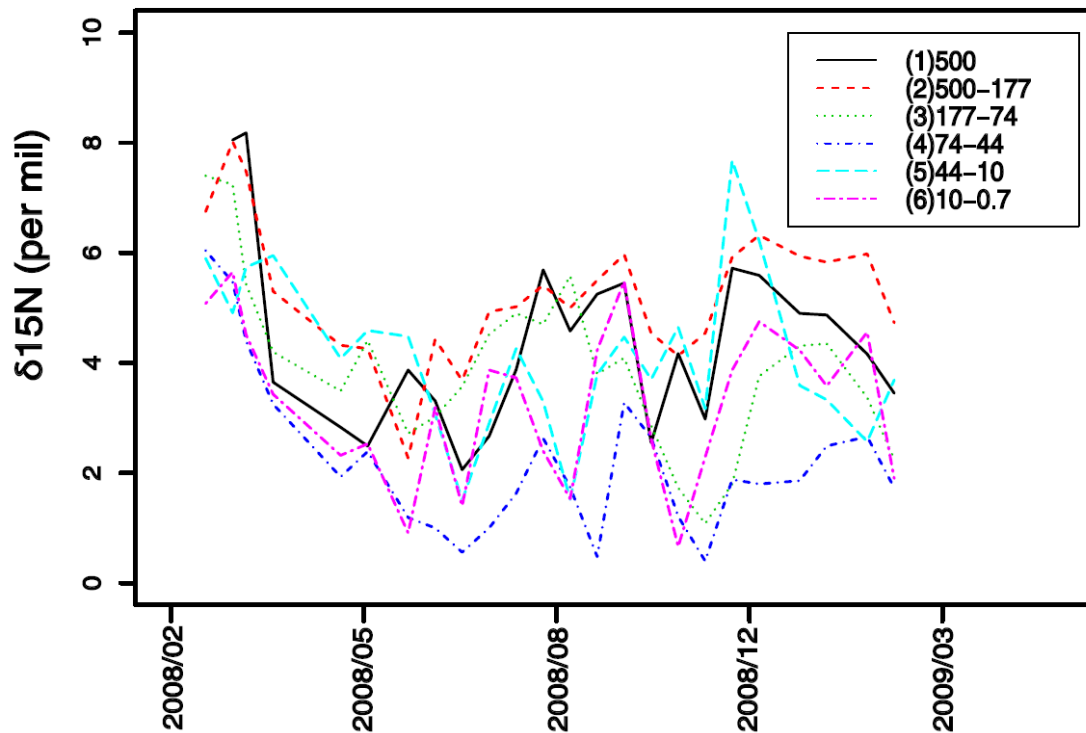


Figure 9 Time series of $\delta^{15}\text{N}$ for all size fractions. The **(4)74-44 μm** and **(6)10-0.7 μm** baselines fraction always show lower $\delta^{15}\text{N}$ value. The $\delta^{15}\text{N}$ values of the **(5)44-10 μm** size fraction were always higher than the **(4)74-44 μm** size fraction.

The time series of $\delta^{13}\text{C}$ signature for all size fractions

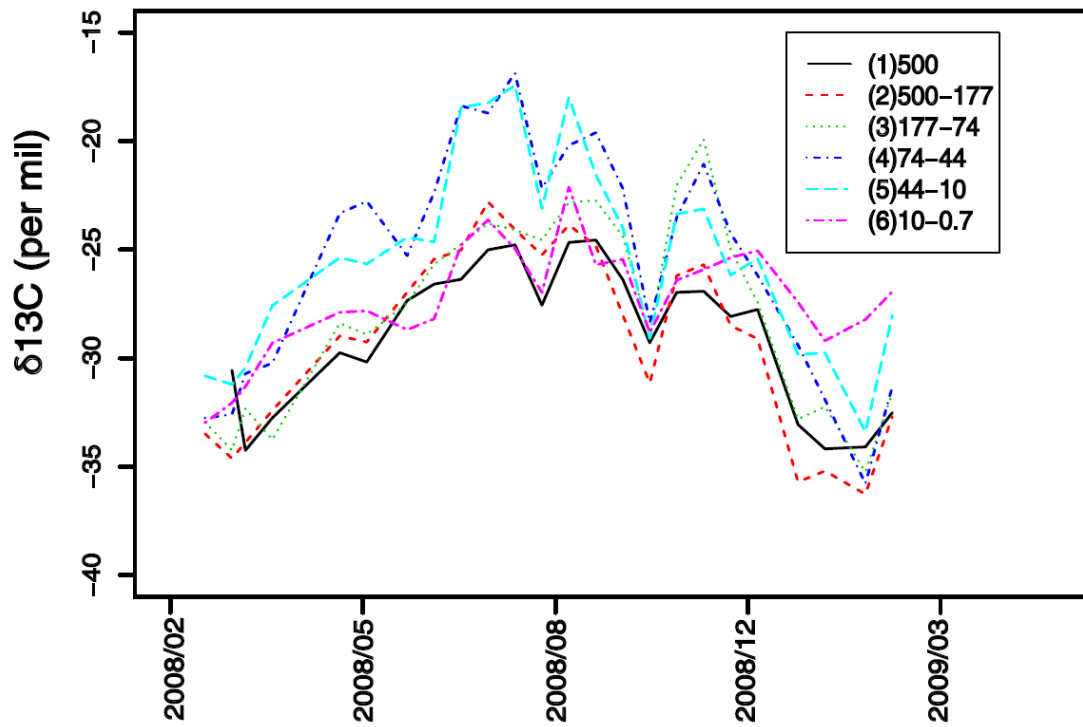
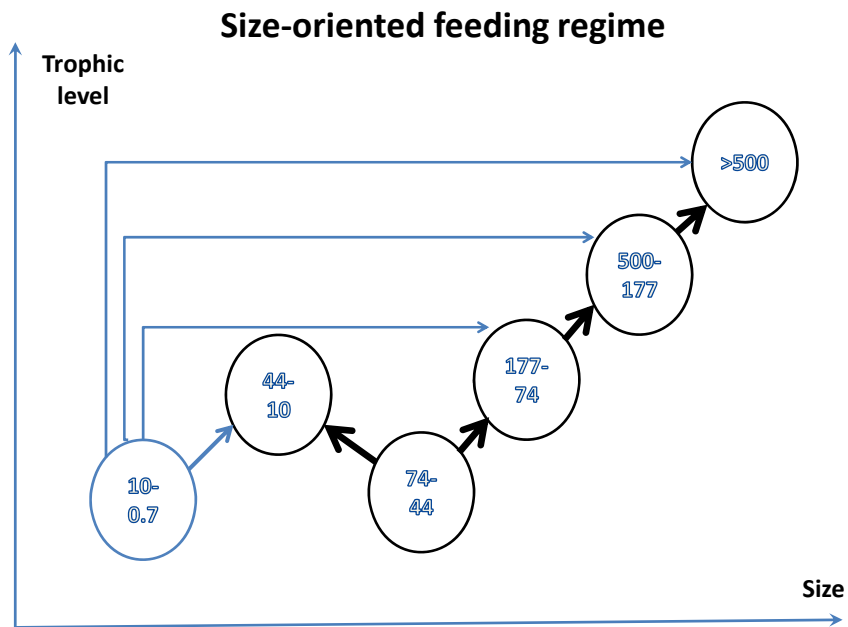


Figure 10 Time series of $\delta^{13}\text{C}$ for all size fractions. The $\delta^{13}\text{C}$ of the **(5)44-10 μm** size fraction have more similar $\delta^{13}\text{C}$ value with the **(4)74-44 μm** baseline fraction, which are mainly composed of larger phytoplankton.

(a)



(b)

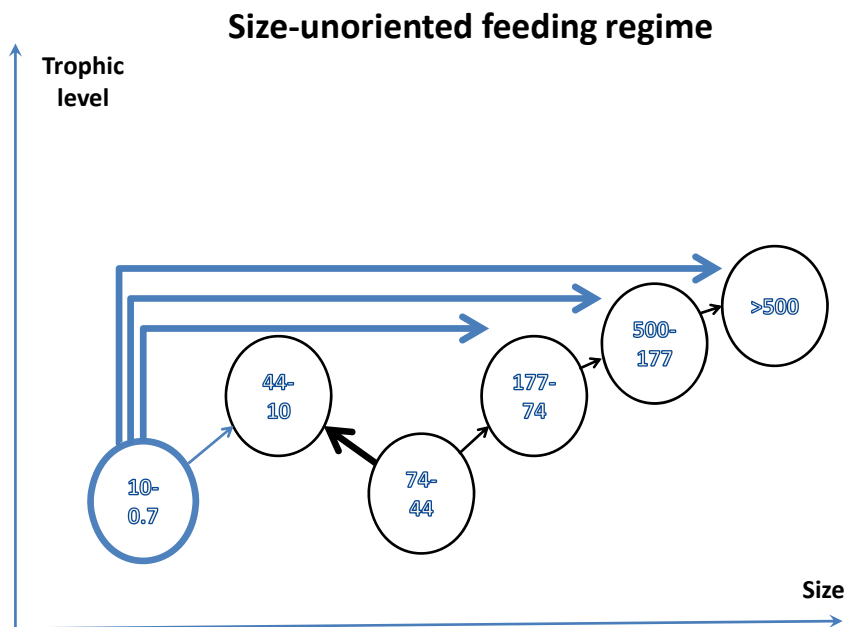


Figure 11 The hypothetical regimes of energetic flow in the Feitsui Reservoir. There is high intensity of omnivorous feeding in size-unoriented feeding regime.

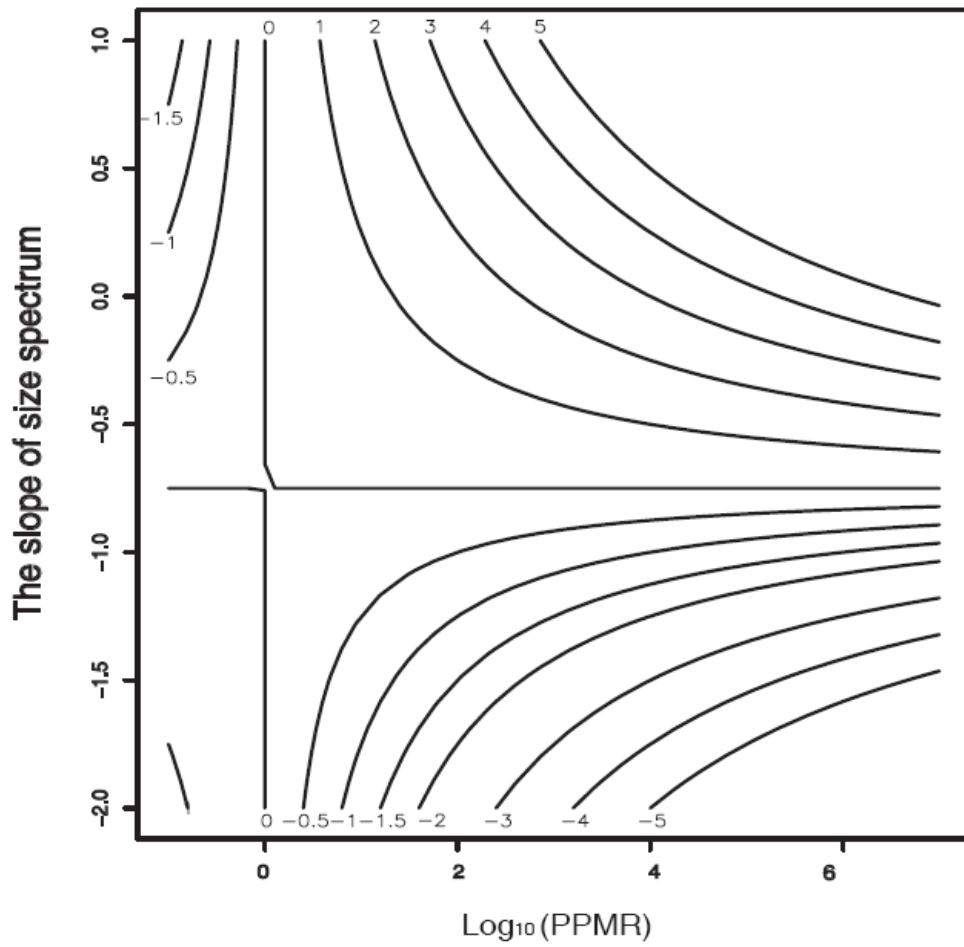


Figure 12 The theoretical relationship among TE, PPMR and the slope of size spectrum. The lines on the contour are TE under the \log_{10} scale.

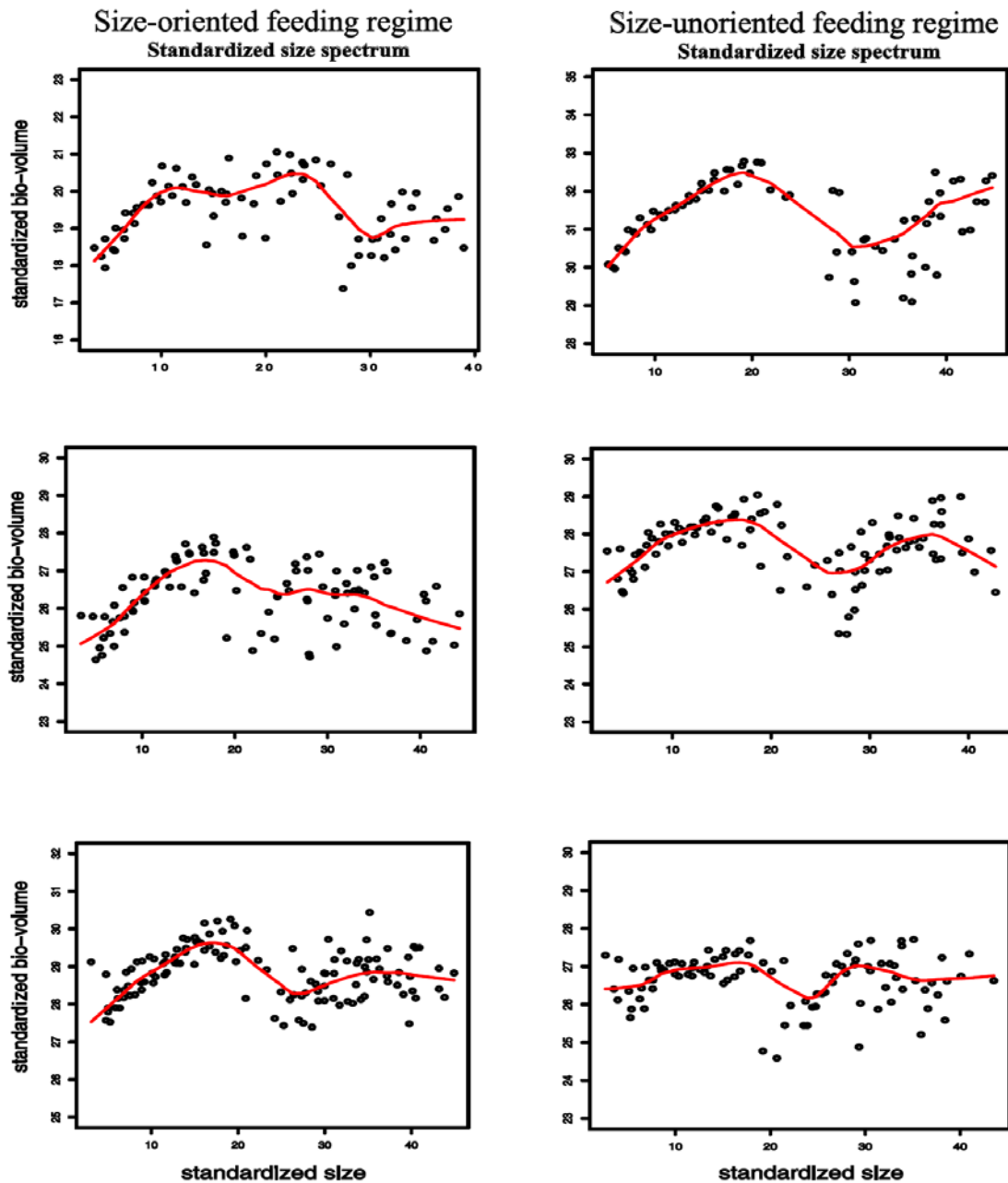


Figure 13 The standardized size spectrum. All size spectra rotate to the slope equal to 0 and mean intercept for each groups determined by K means clustering. The size-TL relationships are not significant in left hand side groups but are significant in right hand side. The clear secondary structures of size spectrum appear in right groups, which mean the non-significance of size-TL relationship might cause the secondary structure of size spectrum.

Table

Table 1 The correspondences between isotope size fractions and their main groups.

From the images from flowCAM analysis and previous suggestion (Wetzel 2001), the main groups constitute each size fraction was list here.

Size fraction	Size range (μ m)	Main groups
(1)	>500	Copepod, Cladocera
(2)	500-177	Larva stage of Crustacean
(3)	177-74	Rotifer, nauplia
(4)	74-44	Larger phytoplankton
(5)	44-10	Ciliate, flagellate
(6)	10-0.7	HNF, bacteria, cyanobacteria

Table 2 The result of K means clustering for each sampling date. Six groups were identified by K means clustering method.

Days	2008/02/26	2008/03/11	2008/03/18	2008/04/01	2008/05/06	2008/05/20
Groups	B	B	B	E	D	D
Days	2008/06/10	2008/06/24	2008/07/08	2008/07/22	2008/08/05	2008/08/19
Groups	D	F	C	C	C	F
Days	2008/09/02	2008/09/16	2008/09/30	2008/10/14	2008/10/28	2008/11/11
Groups	C	F	A	D	F	F
Days	2008/11/25	2008/12/09	2008/12/30	2009/01/13	2009/02/03	2009/02/17
Groups	A	A	E	E	E	E

Table 3 The result of permutation test for canonical redundancy analysis

	Adjusted R2	F	P value	Variation
Whole axis	0.670	3.616	0.028	100%
RDA axis 1	0.772	61.833	0.001	78.069%
RDA axis 2	0.009	1.155	0.273	4.728%



Table 4 Regression coefficients are shown, and PPMR estimated from $\delta^{15}\text{N}$ values and size, estimated TE from metabolic theory for each sampling period.

Date	Intercept	Slope	p (1-tailed)	PPMR	TE	R2
2008/02/26	-1.988	0.174	0.062	743941.600	0.151	0.517
2008/03/11	-2.585	0.190	0.011*	238670.900	3.017	0.754
2008/03/18	-2.467	0.210	0.015*	74089.580	0.300	0.783
2008/04/01	-6.080	0.372	0.439	565.802	0.809	0.015
2008/05/06	-3.992	0.255	0.311	10252.550	0.394	0.044
2008/05/20	-25.868	1.402	0.487	5.372	0.662	0.002
2008/06/10	-2.717	0.222	0.195	40257.190	0.150	0.218
2008/06/24	-1.251	0.105	0.176	6090000000	0.005	0.254
2008/07/08	-2.381	0.173	0.180	810521.700	0.066	0.185
2008/07/22	3.274	-0.155	0.228	<0.001	201.988	0.143
2008/08/05	-14.754	0.821	0.460	17.634	0.315	0.001
2008/08/19	-2.250	0.199	0.003**	139417.000	0.027	0.835
2008/09/02	-3.500	0.276	0.043*	5053.281	0.038	0.603
2008/09/16	-1.279	0.121	0.119	300000000	<0.001	0.333
2008/09/30	0.730	-0.058	0.038*	<0.001	488000000	0.579
2008/10/14	-2.700	0.172	0.362	912621.100	0.000	0.038

Table 4 (continued)

Date	Intercept	Slope	p (1-tailed)	PPMR	TE	R2
2008/10/28	-4.181	0.322	0.103	1514.875	0.030	0.367
2008/11/11	-3.174	0.213	0.323	62231.970	0.007	0.056
2008/11/25	-6.599	0.473	0.206	146.484	0.046	0.144
2008/12/09	-3.632	0.325	0.107	1420.189	0.008	0.361
2008/12/30	-2.289	0.221	0.023*	41955.950	0.005	0.650
2009/01/13	-3.907	0.307	0.023*	2165.327	0.022	0.707
2009/02/03	-3.078	0.204	0.091	105032.400	NA	0.411
2009/02/17	-2.081	0.173	0.073	800370.600	0.032	0.389

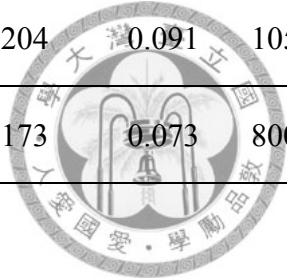


Table 5 Regression coefficients are shown, and PPMR estimated from $\delta^{15}\text{N}$ values

and size, estimated TE from metabolic theory for six K means groups

Group	Intercept	Slope	Pr (1-tailed)	PPMR	TE	slope	R2
A	-4.365	0.310	0.127	0.020×10^5	0.011	-1.340	0.070
B	-2.282	0.189	0.001	2.670×10^5	0.518	-0.803	0.698
C	-0.723	0.089	0.124	3.320×10^{11}	0.000	-1.084	0.067
D	-1.427	0.126	0.133	1400×10^5	0.006	-1.021	0.055
E	-2.288	0.192	0.001	2.100×10^5	0.020	-1.069	0.367
F	-2.212	0.180	0.003	4.713×10^5	0.005	-1.151	0.280



Table 6 The regression coefficients of primary production versus $\delta^{13}\text{C}$ distance

$\delta^{13}\text{C}$ distance	Slope	Std. Error	t value	Pr(> t)
$\Delta^{13}\text{C}_{14}$	0.028	0.009	3.163	0.006
$\Delta^{13}\text{C}_{34}$	0.020	0.007	2.821	0.012
$\Delta^{13}\text{C}_{46}$	0.023	0.008	2.837	0.011
$\Delta^{13}\text{C}_{56}$	0.016	0.007	2.162	0.045



Table 7 Results of permutation test investigating the difference of $\delta^{13}\text{C}$ distance

between groups with and without a significant size-TL relationship

$\delta^{13}\text{C}$ distance difference	Difference	P value	$\alpha=5\%$ lower bound	$\alpha=5\%$ upper bound
$d\Delta^{13}\text{C}_{14}$	-15.656	0.052	-15.814	15.791
$d\Delta^{13}\text{C}_{24}$	-13.395	0.035	-12.549	12.440
$d\Delta^{13}\text{C}_{34}$	-13.663	0.018	-11.720	11.364
$d\Delta^{13}\text{C}_{54}$	1.276	0.305	-2.363	2.291
$d\Delta^{13}\text{C}_{16}$	9.112	0.049	-9.456	9.097
$d\Delta^{13}\text{C}_{26}$	13.749	0.084	-15.241	14.987
$d\Delta^{13}\text{C}_{36}$	15.200	<0.001	-10.387	10.364
$d\Delta^{13}\text{C}_{56}$	-7.851	0.199	-11.317	10.803

Table 8 ANOVA analysis detecting the omnivorous effect of zooplankton

Analysis of variance of the trophic position of zooplankton fractions **>500 μm** , **500-177 μm** and **177-74 μm** in groups with size-TL relationship showing significant trophic difference among zooplanktons

	df	SS	MS	F	P value
Size	2	16.220	8.110	6.729	0.003**
residual	35	41.973	1.199		

Analysis of variance of the trophic position of zooplankton fractions **>500 μm** , **500-177 μm** and **177-74 μm** in groups without size-TL relationship showing equal trophic position among zooplanktons

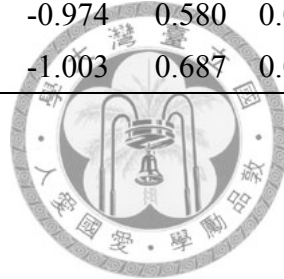
	df	SS	MS	F	P value
Size	2	5.604	2.802	1.093	0.348
residual	30	76.891	2.563		

Table 9 The regression coefficients of size spectrum for each sampling date

Days	Intercept a	Slope b	se.a	se.b	p.a	p.b	R²
2008/02/26	21.263	-0.890	0.798	0.046	<0.001	<0.001	0.937
2008/03/11	16.984	-0.661	0.573	0.035	<0.001	<0.001	0.938
2008/03/18	19.831	-0.857	0.647	0.036	<0.001	<0.001	0.956
2008/03/25	21.023	-0.903	0.386	0.027	<0.001	<0.001	0.984
2008/04/01	20.315	-0.783	0.498	0.029	<0.001	<0.001	0.968
2008/04/08	23.030	-0.937	0.491	0.034	<0.001	<0.001	0.975
2008/04/15	23.130	-0.919	0.680	0.041	<0.001	<0.001	0.955
2008/04/29	22.140	-0.865	0.381	0.026	<0.001	<0.001	0.983
2008/05/06	22.521	-0.851	0.680	0.041	<0.001	<0.001	0.948
2008/05/13	25.424	-0.825	0.305	0.021	<0.001	<0.001	0.988
2008/05/20	26.295	-0.995	0.811	0.048	<0.001	<0.001	0.946
2008/06/03	28.117	-1.036	0.427	0.030	<0.001	<0.001	0.985
2008/06/10	25.468	-0.929	0.542	0.032	<0.001	<0.001	0.972
2008/06/17	25.949	-0.897	0.221	0.015	<0.001	<0.001	0.994
2008/06/24	26.787	-0.989	0.608	0.036	<0.001	<0.001	0.969
2008/07/01	28.576	-1.104	0.514	0.036	<0.001	<0.001	0.981
2008/07/08	26.959	-0.950	0.557	0.033	<0.001	<0.001	0.972
2008/07/15	29.113	-1.131	0.726	0.050	<0.001	<0.001	0.964
2008/07/22	27.229	-1.099	0.784	0.045	<0.001	<0.001	0.959
2008/07/29	29.217	-1.183	0.699	0.048	<0.001	<0.001	0.969
2008/08/05	27.961	-1.153	1.029	0.064	<0.001	<0.001	0.935
2008/08/12	28.740	-1.179	0.801	0.056	<0.001	<0.001	0.959
2008/08/19	26.833	-1.055	0.818	0.049	<0.001	<0.001	0.951
2008/08/26	27.454	-1.056	0.626	0.043	<0.001	<0.001	0.969
2008/09/02	27.808	-1.133	0.916	0.055	<0.001	<0.001	0.947
2008/09/09	27.734	-1.070	0.657	0.046	<0.001	<0.001	0.967
2008/09/16	29.502	-1.288	1.035	0.064	<0.001	<0.001	0.946
2008/09/23	29.193	-1.191	0.651	0.045	<0.001	<0.001	0.973
2008/09/30	29.487	-1.242	0.946	0.058	<0.001	<0.001	0.952
2008/10/07	31.768	-1.379	0.613	0.043	<0.001	<0.001	0.982
2008/10/14	31.800	-1.310	0.425	0.026	<0.001	<0.001	0.992
2008/10/21	28.230	-1.019	0.593	0.041	<0.001	<0.001	0.970

Table 9 cont'd

Days	Intercept a	Slope b	se.a	se.b	p.a	p.b	R²
2008/10/28	30.271	-1.228	0.825	0.048	<0.001	<0.001	0.964
2008/11/04	30.620	-1.222	0.799	0.055	<0.001	<0.001	0.962
2008/11/11	29.848	-1.197	0.839	0.050	<0.001	<0.001	0.960
2008/11/25	32.011	-1.367	1.193	0.071	<0.001	<0.001	0.939
2008/12/02	32.265	-1.365	0.795	0.055	<0.001	<0.001	0.970
2008/12/09	31.651	-1.411	1.488	0.092	<0.001	<0.001	0.911
2008/12/16	31.279	-1.357	0.899	0.062	<0.001	<0.001	0.961
2008/12/23	30.291	-1.304	0.752	0.052	<0.001	<0.001	0.970
2008/12/30	29.404	-1.246	1.158	0.071	<0.001	<0.001	0.930
2009/01/13	28.843	-1.245	1.177	0.070	<0.001	<0.001	0.929
2009/02/10	26.925	-0.958	0.526	0.038	<0.001	<0.001	0.972
2009/02/17	25.872	-1.003	0.893	0.053	<0.001	<0.001	0.937
2009/02/24	26.321	-0.974	0.580	0.040	<0.001	<0.001	0.969
2009/03/03	27.133	-1.003	0.687	0.048	<0.001	<0.001	0.959



Reference

- Azam, F., T. Fenchel, J. G. Field, J. S. Gray, L. A. Meyer-Reil, and F. Thingstad. 1983. The ecological role of water-column microbes in the sea. *Marine Ecology Progress Series* **10**:257-263.
- Barabasi, A. L. and R. Albert. 1999. Emergence of scaling in random networks. *Science* **286**:509.
- Belgrano, A. 2005. *Aquatic food webs: an ecosystem approach*. Oxford University Press, USA.
- Brendelberger, H. 1991. Filter mesh size of cladocerans predicts retention efficiency for bacteria. *Limnology and Oceanography* **36**:884-894.
- Brown, J. H. and J. F. Gillooly. 2003. Ecological food webs: High-quality data facilitate theoretical unification. *Proceedings of the National Academy of Sciences* **100**:1467-1468.
- Brown, J. H., J. F. Gillooly, A. P. Allen, V. M. Savage, and G. B. West. 2004. Toward a metabolic theory of ecology. *Ecology* **85**:1771-1789.
- Cairns, J., P. McCormick, and B. Niederlehner. 1993. A proposed framework for developing indicators of ecosystem health. *Hydrobiologia* **263**:1-44.
- Cohen, J. E., F. Briand, C. M. Newman, and Z. J. Palka. 1990. *Community food webs: data and theory*. Springer-Verlag.
- Cohen, J. E., T. Jonsson, and S. R. Carpenter. 2003. Ecological community description using the food web, species abundance, and body size. *Proceedings of the National Academy of Sciences* **100**:1781-1786.
- Damuth, J. 1981. Population density and body size in mammals. *Nature* **290**:699-700.
- Gaedke, U. 1993. Ecosystem analysis based on biomass size distributions: a case study of a plankton community in a large lake. *Limnology and Oceanography* **38**:112-127.
- Gillooly, J. F., J. H. Brown, G. B. West, V. M. Savage, and E. L. Charnov. 2001. Effects of size and temperature on metabolic rate. *Science* **293**:2248-2251.
- Hannides, C. C. S., B. N. Popp, M. R. Landry, and B. S. Graham. 2009. Quantification of zooplankton trophic position in the North Pacific Subtropical Gyre using stable nitrogen isotopes. *Limnology and Oceanography* **54**:50-61.
- Heath, M. R. 1995. Size spectrum dynamics and the planktonic ecosystem of Loch Linnhe. *ICES Journal of Marine Science* **52**:627-642.
- Jennings, S., J. K. Pinnegar, N. V. C. Polunin, and K. J. Warr. 2002a. Linking size-based and trophic analyses of benthic community structure. *Marine Ecology Progress Series* **226**:77-85.
- Jennings, S., K. J. Warr, and S. Mackinson. 2002b. Use of size-based production and

- stable isotope analyses to predict trophic transfer efficiencies and predator-prey body mass ratios in food webs. *Marine Ecology Progress Series* **240**:11-20.
- Kerr, S. R. and L. M. Dickie. 2001. *The biomass spectrum*. Columbia University Press.
- Kerr, S. R. and R. A. Ryder. 1988. The applicability of fish yield indices in freshwater and marine ecosystems. *Limnology and Oceanography* **33**:973-981.
- Knoechel, R. and L. Holtby. 1986. Cladoceran filtering rate: body length relationships for bacterial and large algal particles. *Limnology and Oceanography* **31**:195-200.
- Kuo, J. T., W. C. Liu, R. T. Lin, W. S. Lung, M. D. Yang, C. P. Yang, and S. C. Chu. 2003. Water quality modeling for the Feitsui Reservoir in Northern Taiwan. *Journal of the American Water Resources Association* **39**:671-687.
- Legendre, P. 1998. *Numerical ecology*. Elsevier Science.
- Modenutti, B. E. and E. G. Balseiro. 1994. Zooplankton size spectrum in four lakes of the Patagonian Plateau. *Limnologica* **24**:51-56.
- Montoya, J. and R. Sole. 2002. Small world patterns in food webs. *Journal of theoretical biology* **214**:405-412.
- Peters, R. H. 1986. *The ecological implications of body size*. Cambridge University Press.
- Peterson, B. J., J. E. Hobbie, and J. F. Haney. 1978. Daphnia grazing on natural bacteria. *Limnology and Oceanography* **23**:1039-1044.
- Platt, T. and K. L. Denman. 1978. *The structure of pelagic marine ecosystems*. Marine Ecology Laboratory, Bedford Institute of Oceanography.
- Post, D. M. 2002. Using stable isotopes to estimate trophic position: models, methods, and assumptions. *Ecology* **83**:703-718.
- San Martin, E., X. Irigoien, R. P. Harris, A. Lopez-Urrutia, M. V. Zubkov, and J. L. Heywood. 2006. Variation in the transfer of energy in marine plankton along a productivity gradient in the Atlantic Ocean. *Limnology and Oceanography* **51**:2084-2091.
- Sheldon, R. W., A. Prakash, and W. H. Sutcliffe Jr. 1972. The size distribution of particles in the ocean. *Limnology and Oceanography* **17**:327-340.
- Silvert, W. and T. Platt. 1978. Energy flux in the pelagic ecosystem: a time-dependent equation. *Limnology and Oceanography* **23**:813-816.
- Sprules, W. and J. Bowerman. 1988. Omnivory and food chain length in zooplankton food webs. *Ecology* **69**:418-426.
- Sprules, W. G., S. B. Brandt, D. J. Stewart, M. Munawar, E. H. Jin, and J. Love. 1991. Biomass size spectrum of the Lake Michigan pelagic food web. *Canadian*

- Journal of Fisheries and Aquatic Sciences **48**:105-115.
- Sprules, W. G. and M. Munawar. 1986. Plankton size spectra in relation to ecosystem productivity, size, and perturbation. Canadian Journal of Fisheries and Aquatic Sciences **43**:1789-1794.
- West, G. B., J. H. Brown, and B. J. Enquist. 1997. A general model for the origin of allometric scaling laws in biology. Science **276**:122-126.
- Wetzel, R. 2001. Limnology: lake and river ecosystems. 3 edition. Academic Press.
- White, E. P., S. K. M. Ernest, A. J. Kerkhoff, and B. J. Enquist. 2007. Relationships between body size and abundance in ecology. Trends in Ecology & Evolution **22**:323-330.
- Wu, J. T. and J. W. Chou. 1998. Dinoflagellate associations in Feitsui Reservoir, Taiwan. Bot Bull Acad Sin **39**:137-145.



Appendix

Derivation TE, size spectrum, PPMR relationship

According to metabolic theory, the production of each trophic level could be

expressed as $iNM^{3/4}e^{-E/kT}$. Therefore, TE could be expressed by

$$TE = i_{j+1} N_{j+1} M_{j+1}^{3/4} e^{-E/kT} / i_j N_j M_j^{3/4} e^{-E/kT}$$

Where M_j means the body size of trophic level j and N_j means the abundance of

trophic level j . By assuming constant normalized factors, TE could be simplified to

the following form:

$$TE = N_{j+1} M_{j+1}^{3/4} / N_j M_j^{3/4}$$



Let τ denote the trophic level of size M . The ratio of M_{j+1} to M_j , M_{j+1} / M_j , is equal to

$(PPMR)^\tau$. And τ can be represented as the function of PPMR and M as following:

$$\tau = \log_{PPMR}(M / M_0) = \log (M / M_0) / \log (PPMR)$$

The total rate of metabolism of all size M individuals, I_{tot} , could be expressed as

following:

$$I_{tot} = (i_0 N_0 M_0^{3/4} e^{-E/kT}) TE^\tau$$

By substituting τ with the function of PPMR and M in I_{tot} and dividing total

metabolic rate I_{tot} by individualistic metabolic rate I , we can show that the abundance

is scaled by body size with the exponent equal to $\beta = (\log TE / \log PPMR) - 0.75$,

that is the slope of size spectrum

$$N = I_{tot} / I = N_0 (M / M_0)^{[\log (TE) / \log (PPMR)] - 0.75} \text{----- (1)}$$

By rearranging the predictive formula of the slope of size spectrum β , the TE could be represented by the following formula:

$$TE = PPMR^{(\beta + 0.75)} \text{----- (2)}$$

The predicted slope of size spectrum could be consistent with previous hypothesis (Platt 1977) if the 10% TE and 10^4 PPMR be assumed. However, these assumptions are still under debate, especially TE, it should be checked further.

